ISSN 1069-3513, Izvestiya, Physics of the Solid Earth, 2010, Vol. 46, No. 6, pp. 544–554. © Pleiades Publishing, Ltd., 2010.
Original Russian Text © A.A. Lyubushin, 2010, published in Fizika Zemli, 2010, No. 6, pp. 86–96.

# The Statistics of the Time Segments of Low-Frequency Microseisms: Trends and Synchronization

**A. A. Lyubushin**

*Institute of Physics of the Earth, Russian Academy of Sciences, ul. Bol'shaya Gruzinskaya 10, Moscow, 123995 Russia*

Received September 17, 2009

**Abstract**—The problem of identifying the effects of synchronization in the parameters of low-frequency microseismic noise from the data of 77 stations belonging to the F-net broadband seismograph network in Japan for the period from the beginning of 1997 through August, 2009 is considered. The vertical components measured initially with a sampling rate of one second and subsequently converted into the signals sampled at 1 minute intervals by means of averaging and decimation are used in the analysis. Six statistics are taken as the parameters: the support width of the multifractal singularity spectrum; the generalized Hurst exponent; the asymmetry coefficient of the spectrum of singularity; the logarithmic variance; the spectral exponent; and the linear predictability index. These parameters are calculated from the realizations contained within consecutive daily time intervals. When using the moving time window with a width of one year for evaluating the multiple correlation, the daily variations in the median values of the statistics of the noise measured at five spatial clusters of stations exhibit a stable increase in the synchronization not long before the Hokkaido earthquake (September 25, 2003; $M = 8.3$), subsequently passing to the new level of high synchronization. Based on the analysis of the trends in the index of linear predictability it turned out possible to estimate the beginning of the enhancement in the synchronization with rather high accuracy as the middle of 2002. The effect revealed for the variations in the different parameters of microseisms is an independent argument for the earlier conclusion about the synchronization in the field of the microseismic noise on the Japan Islands.

**DOI:** 10.1134/S1069351310060091

## INTRODUCTION

The main source of energy for the low-frequency microseismic vibrations with periods from several tens of seconds to a few hundreds of minutes is the variations in the atmospheric pressure and the impact of oceanic waves on the coast and the shelf. Vibrations with periods ranging from 5 to 500 seconds are generated mainly by the oceanic waves, whereas in the interval of periods from 10 to 300 minutes, the main source of energy is the direct effect of the air pressure fluctuations. One of the pioneer works, which pointed to the distinct correlation between the low-frequency microseisms with the atmospheric processes, is the paper by Gutenberg [1947]. He proposed using the information about microseismic fluctuations for real-time weather prediction. Later on, this correlation was the subject of repeated studies by many authors [Lin'kov, 1987; Lin'kov et al., 1990; Friedrich et al., 1998; Kobayashi and Nishida, 1998; Tanimoto et al., 1998; Tanimoto and Urn, 1999; Ekstrom, 2001; Tanimoto, 2001; 2005; Berger et al., 2004; Kurrle and Widmer-Schnidrig, 2006; Stehly et al., 2006]. In the works [Rhie and Romanowicz, 2004; 2006], a significant correlation between the intensity of seismic vibrations having periods of approximately four minutes and the height of waves in the oceans is revealed; it was shown that this intensity is independent of the seismic activity of the Earth. The suggested possible mechanism of generation of such vibrations is the disturbance in the gravity field caused by high waves and the subsequent excitation by these waves of the low-frequency seismic waves at the bottom of the ocean. The North Pacific Ocean in winter and the South Atlantic Ocean in summer are proposed as the main places of the emergence of such vibrations.

In spite of the fact that the main source of energy for low-frequency microseisms is an external one with respect to the Earth's crust, and the latter is merely the propagation medium, the conditions in the Earth's crust affect the statistical characteristics and the specific features in the behavior of low-frequency microseismic vibrations. Consequently, if we study the time variations of the characteristics of seismic noise, this study will hopefully yield important information concerning the changes in the Earth's crust, including those linked with the seismic process and with the preparation of strong earthquakes. The specific features in the periodic structure of the point process, generated by strong bursts of microseismic noise before strong earthquakes, were investigated in [Sobolev, 2004; Sobolev et al., 2005]. Further, the analysis of the periodic structure of the bursts was substantially extended by studying the intensity and energy of asymmetric low-frequency pulses in the seismic noise [Sobolev and Lyubushin, 2006; Sobolev et al., 2008; Sobolev, 2008].

Another challenging trend in analyzing the specificity of low-frequency seismic noise is studying the effects of the enhancement in the synchronization in the microseismic field. This approach evidently requires the use of synchronous data from several seismic stations. When studying the noise before the catastrophic earthquake in Sumatra (December 26, 2004; $M = 9.2$), the authors of the work [Sobolev and Lyubushin, 2007] used the multidimensional spectral and wavelet measures of coherence estimated in the moving time windows [Lyubushin, 2007] for this purpose. The measures of coherence were evaluated for microseisms after the transition to the sampling rate of 30 seconds (via averaging by 600 times the initial broad-band seismic data of the IRIS network samples at 20 Hz) within a relatively narrow time window with a length of 12 hours. A significant effect of synchronization appeared at four seismic stations (including those, which are quite remote from the epicenter) two and a half days prior to the revelation of the main shock; moreover, the shift of the fundamental period of synchronization towards low frequencies (from a period of 2.5 minutes to 6 minutes) was observed as the right end of the moving time window approached the earthquake onset time. This effect of synchronization with the accompanying migration of the fundamental frequency was interpreted as the impact of the earthquake at Macquarie Island (the southernmost margin of Tasmania, December 23, 2004, $M = 7.9$), which could have served as a trigger for the Sumatra catastrophe.

Further attempts to apply the measures of coherence directly to the seismic data resulted only in the identification of the obvious and trivial effects of synchronization associated either with the arrivals of seismic waves from strong earthquakes (in the high-frequency range), or with the global tidal effect on the broadband seismic data (in the low-frequency range with wide time windows used). In this connection, the idea appeared to make a preliminary nonlinear conversion of the initial time series into an array of the dimensionless parameters, each of which would be calculated at particular time intervals with a "small" length and would contain information about the statistical properties of the noise. It was decided to use the parameters of the multifractal spectrum of singularity $F(\alpha)$ [Feder, 1988], namely, the width of the spectrum support $\Delta\alpha$, and the argument value $\alpha^*$, at which the spectrum $F(\alpha)$ reaches its maximum ($\alpha^*$ is also called a generalized Hurst exponent) as such an informative nonlinear transformation of the initial data. The use of the estimates for the spectra of singularity of the noise component contained in the time series is one of the promising trends in the data analysis in different fields of monitoring, including geophysical monitoring [Kantelhardt et al., 2002; Ida et al., 2005; Currenti et al., 2005; Ramirez-Rojas et al., 2005; Telesca et al., 2005; Lyubushin and Sobolev, 2006; Lyubushin, 2007; 2008; 2009].

Due to the transition from the analysis of the initial data on low-frequency microseisms to the study of the variations in the parameters $\Delta\alpha$ and $\alpha^*$ of their spectra of singularity, estimated in consecutive "short" time windows (which is at the same time, in fact, also a transition to a lower frequency range), it became possible to reveal the latent effects of synchronization, which could not be identified by analyzing the initial data [Lyubushin and Sobolev, 2006; Lyubushin, 2007; 2008; 2009]. The length of the "small" moving time window, within which the spectra of singularity were evaluated, was 12 hours (upon the transition to the half-minute sampling of microseisms) by shifting the time window by one hour. The influence of the low-frequency tidal variations was eliminated by removing the local polynomial scale-dependant trends in each window [Lyubushin, 2007]. The spectral measures of coherence for the variations in the parameters of the spectra of singularity were evaluated in the moving time windows with a length of 5 days. This resulted in the identification of the effects of synchronization, which preceded the earthquakes in Kamchatka (the Kronotskii earthquake of December 5, 1997; $M = 7.8$) and, also, in Japan (not far from Hokkaido, on September 25, 2003, $M = 8.3$). The effects of synchronization have periods ranging from 250 to 1000 minutes and appear 3–7 days prior to the event [Lyubushin and Sobolev, 2006; Sobolev et al., 2008; Lyubushin, 2008]. However, contrary to expectations, the application of this approach to the analysis of microseisms preceding the Simushirskoe earthquake on the Kurile Islands (November 15, 2006; $M = 8.2$) did not result in the expected effect of antecedent synchronization. Furthermore, this earthquake was preceded by the stable absence of synchronization; at the same time, the burst of synchronous behavior was identified for a time segment with a duration of about 16 days (October 11, 2006–October 28, 2006); within this time interval, the fine frequency–time structure of the spot of synchronization was rather stable with respect to the variations in the set of stations, included in the data processing [Lyubushin, 2008]. The duration of the analyzed time intervals before the three aforementioned events was 30.5, 25, and 61.5 days, respectively; and the number of stations analyzed simultaneously was 6, 6, and 8, respectively. The stations were spaced from 70 to 7160 km from the epicenter of a particular earthquake.

One of the most probable reasons for the large span of the effects of synchronization is the intense atmospheric and oceanic processes occurring not only in the neighborhood of the measurement sites, but practically in any region of the world. These processes can either synchronize the noise parameters or trigger strong earthquakes. Thus, the episodes of synchronization observed before the Kronotskii earthquake on November 5, 1997 and before the Hokkaido earthquake on September 25, 2003, might be indications of the trigger action on the Earth's crust of atmospheric and oceanic processes, which simultaneously synchronize the variations in the parameters of microseismic noise.

In relation to this hypothesis, it is interesting to trace how the degree of synchronization in the microseism changes in time as a result of the atmospheric action. In other words, if the parameters of microseism are synchronized by a strongly correlated atmospheric process, then, depending on the crustal conditions, the degree of this synchronization can be either low or high. The practical implementation of this idea requires analyzing seismic records over a period of years rather than a short duration of 20–60 days; and, the time window, which is used for evaluating a singularity spectrum (or other statistics of the time interval), must also be much wider than 5 days.

The database of broad-band seismic records of the F-net network, which consists of 83 stations located on the Japan islands, and has been in operation since the beginning of 1997 until currently, is almost ideal for this purpose. The data of this network are accessible for free downloading on the Internet (http://www.hinet.bosai.go.ip/fnet) and have a fast and convenient interface. In the work [Lyubushin, 2009], the LHZ-records of the vertical components of the F-net data sampled at 1 Hz were analyzed for the period from the beginning of 1997 through June, 2008. Also, signals sampled at 1 min intervals were considered. These data series were obtained by averaging and decimation of the initial data. Estimation of the multi-fractal spectra of singularity in sequential time windows with a length of 30 minutes for 1 s data and in windows with a length of one day for 1 min data, revealed long-period trends in the variations in the width of the support of singularity spectrum $\Delta\alpha$ and in the generalized Hurst exponent $\alpha^*$ of the low-frequency microseismic field. The average value of the parameter $\Delta\alpha$ for 1 s data noticeably decreases before the Hokkaido earthquake of September 25, 2003, $M = 8.3$, and does not return to its previous level. For the 1 min data, the variations in $\alpha^*$ before September, 2003 were subjected to strong annual variations, which had completely vanished later on. Both these effects are interpreted as the increase in the synchronization of microseismic noise at the Japan islands after the earthquake of September 25, 2003. This hypothesis is also confirmed by the estimates of the measure of correlation and the spectral measure of coherence between the changes in the mean values of $\Delta\alpha$ and $\alpha^*$, calculated for the one-minute data within five spatial clusters of stations from consecutive time segments with a length of two months. On the basis of the known statement in the theory of catastrophe, which declares that synchronization is one of the flags indicative of an impending catastrophe [Gilmore, 1981], one can assume that the event on Hokkaido might be a foreshock of an even stronger earthquake, which is being prepared in the region of the Japan islands.

The present work is the continuation of the paper [Lyubushin, 2009]. It includes the analysis of one more year of continuous observations, and, in addition, it is aimed at checking whether it is true that the synchronization in the statistics of low-frequency microseisms should be observed not only for the parameters of the spectrum of singularity (to which, besides $\Delta\alpha$ and $\alpha^*$, another parameter is added, namely, the index of asymmetry of the spectrum of singularity $\gamma$), but also for the other characteristics of the noise. The latter include the logarithmic variance, the spectral exponent, and a new characteristic, namely, the index of linear predictability. It turned out that, when a very long (with the length of one year) time window is used for evaluating a multidimensional measure for the correlation between the daily variations in the median values of the statistics of the noise from the five spatial clusters, a stable increase in the degree of synchronization is observed not long before the Hokkaido earthquake with the attainment of a new high level of synchronization. In addition, based on the analysis of the trends in the index of linear predictability, it was possible to determine with sufficiently high accuracy the onset of the enhancement in synchronization (the middle of 2002).

## THE USED DATA: F-NET NETWORK

The data of the Japanese broad-band seismic F-net network obtained since the beginning of 1997 to August, 2009 inclusively, which is more than 12.5 years in total, were used in the analysis. The total number of stations was 83, but the number of working stations actually involved in the analysis varied due to the gaps in the data recording, as well as to the closure of old stations and opening of new ones. In the beginning of the operation of the network in 1997, the number of stations was only 17 altogether. Later on, new stations were put into operation (most of all in 2001), but, at the same time, some stations, which were working in the initial period, were closed. The data being analyzed are the vertical components sampled at one second intervals; they contain intervals of data gaps and corrupted data (such as data with all zero values), which is due to the failure in the measuring and recording instrumentation.

Only the stations located at latitudes higher than 30°N were considered. This excludes from the analysis six isolated stations, located on small, remote islands. The location of the remaining 77 stations are presented in Fig. 1 by the numbers from 1 to 5, which mark the belonging of the stations to the 5 spatial clusters; also

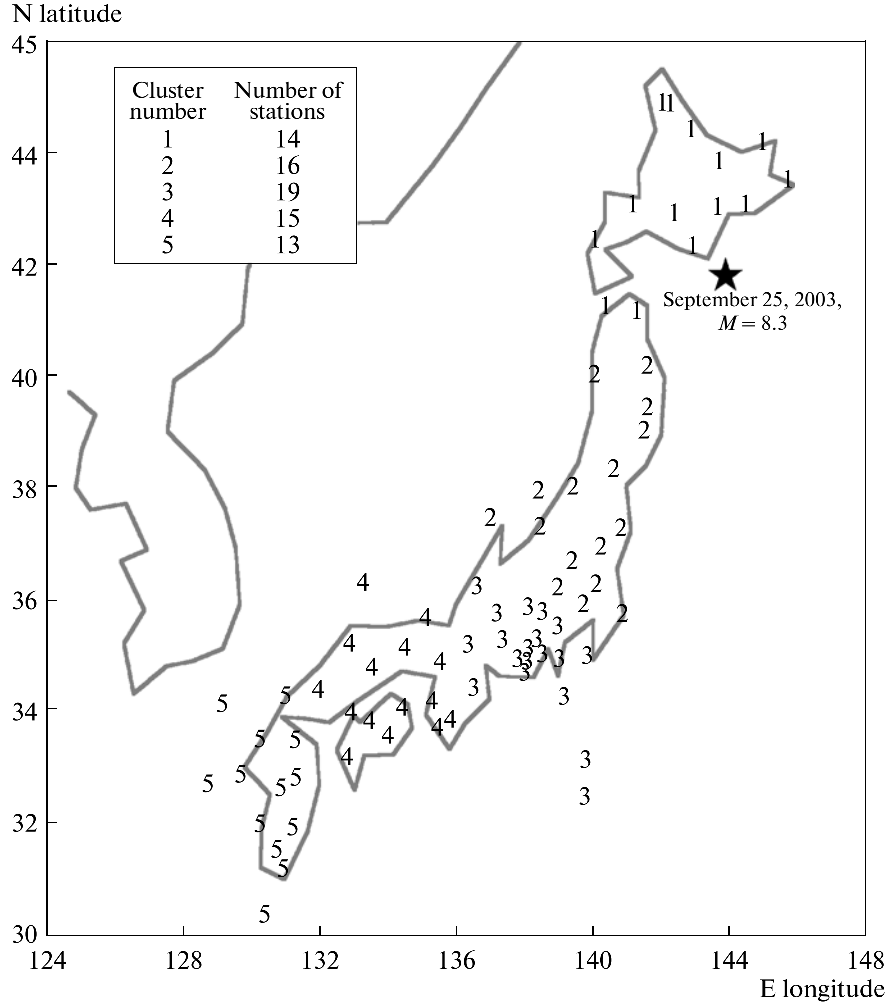


**Fig. 1.** The locations of 77 broad-band seismic stations of the F-net network and their grouping into five spatial clusters, with an indication of the number of stations in each cluster. The hypocenter of the earthquake of September 25, 2003, $M = 8.3$, is shown by the star.

indicated is the number of stations in each cluster. The grouping of stations into spatial clusters is done for the sake of spatial averaging of the parameters of microseims (by calculating the median value over the stations) and for ensuring the continuity of the value averaged over the cluster due to sufficiently large number of stations (i.e., there were always several operating stations in the cluster). The hypocenter of the earthquake of September 25, 2003, $M = 8.3$, is shown by the star.

## THE STATISTICS AND THE METHODS APPLIED

Further in the text, the term "statistics" will be understood as a "function of observations" [Cox and Hinkley, 1974]. Hereinafter, six such statistics will be considered, each of which is determined at consecutive (nonintersecting) time intervals of a given length. For the microseismic data reduced to 1-minute sampling, the length of these time intervals is 24 hours (1440 readings). The records of microseismic vibrations contain gaps and corrupted segments of different length; therefore, in order to obtain a continuous time series of variations in the statistics with a time step of 24 hours, the median value was calculated for those stations, where neither interruptions nor failures occurred in the recording during a given day.

Thus, a set of 30 time series (six parameters, multiplied by five clusters of stations) with a uniform sampling interval of 24 hours was obtained. Each element of each of these 30 time series is the result of three operations of averaging: (1) direct time averaging, i.e., resampling the initial one-second data series into a one-minute data series by calculating the averages over 60 consecutive points; (2) indirect time averaging, implemented by estimating the particular statistics over 1440 consecutive one-minute values of microseisms from each station (if such data are available); (3) the space averaging of the obtained daily estimates of the statistics by calculating the median values over the values from the normally operating stations of a cluster.

**Spectral exponent β and the logarithmic variance log(*Var*).** The spectral exponent β defines the type of variations in the logarithmic power spectrum depending on the logarithmic period; its value is closely related to the fractal characteristics of the noise [Feder, 1988]. The analysis of changes in the spectral exponents is widely used in geophysics [Smirnov et al., 2005]. Below, instead of the classical estimates for the power spectrum, based on the Fourier series expansion or on parametric models, its estimate based on the rate of change of the average squared absolute values of the wavelet coefficients was used [Mallat, 1997]. This by itself provides considerable smoothing of the spectrum, which is necessary for evaluating the spectral exponent:

$$W_k = \sum_{j=1}^{N^{(k)}} \left|c_j^{(k)}\right|^2 / N^{(k)}. \qquad (1)$$

Here, $c_j^{(k)}$ are the coefficients of the orthogonal discrete wavelet expansion of a sample of the time series and $k = 1, \ldots, m$ is the number of the granularity level of the expansion; and $N^{(k)}$ is the number of wavelet coefficients at the level of granularity $k$, $N^{(k)} \leq 2^{(m-k)}$. Then, similarly to the relationship for the rate of growth of the power spectrum, $W_k \sim (s_k)^{\beta}$, where $s_k$ is the characteristic time scale for the detail level $k$. Since $s_k = 2^k–2^{(k+1)}$, then

$$\log_2(W_k) \sim k^{\beta}. \qquad (2)$$

Thus, the slope of the straight line, fitted by the least square method to the pairs of values $((\log_2(W_k)), k)$, gives an estimate for β. The parameter β was evaluated in consecutive time windows with a length of 1440 readings (24 hours). Earlier, this method of calculation of the spectral exponents when analyzing microseismic noise was applied in [Lyubushin, 2008]. In order to eliminate the effect of tidal variations, the polynomial trend of the eighth order was removed in each window; and the wavelet power spectrum (1) and the decimal logarithmic variance log(*Var*) were calculated for the remainder. In this case, the optimal orthogonal Daubechies wavelet with 2 to 10 vanishing moments was selected, which minimizes the entropy of the distribution of the squared wavelet coefficients for the first seven levels of detail of the wavelet expansion (the time scales, or the "periods" are from two to 256 minutes with a time step of one minute).

Above, the parameters are described, which are calculated for the daily time intervals at each station, which provides normal recording for the current day. Further, the procedure of averaging over the stations within a cluster is applied. I designate the median values as $\bar{\beta}_r(s)$ and $\overline{\log(Var)}_r(s)$. In these designations, the overline indicates spatial averaging (calculation of the median within the clusters), the subscript $r = 1, \ldots, 5$ indicates the particular cluster (one of five) to which the value of the median relates, and the argument $s$ is the integer index, which enumerates the consecutive days counting either from the overall beginning of observations (the beginning of 1997), or from the beginning of the time window, in contrast to the time index $t$, which enumerates the consecutive one-minute readings of the seismic records within the current day.

**The index of linear predictability ρ** is calculated as $\rho = V_0/V_{AR} - 1$. Here, $V_0$ is the variance of the error $\varepsilon_0(t+1)$ of the trivial one-step-ahead prediction $\hat{x}_0(t+1)$ for the increments $x(t)$ of seismic records, which is equal to the average over the previous "small" time window with a length of $n$ counts: $\hat{x}_0(t+1) = \sum_{s=t-n+1}^{t} x(t)/n$. Thus, $\varepsilon_0(t+1) = x(t+1) - \hat{x}_0(t+1)$, and $V_0 = \sum_{t=n+1}^{N} \varepsilon_0^2(t)/(N-n)$, where $N > n$ is the number of elements within consecutive "large" time segments. The value of $V_{AR}$ is calculated by a similar formula $V_{AR} = \sum_{t=n+1}^{N} \varepsilon_{AR}^2(t)/(N-n)$, where $\varepsilon_{AR}(t+1) = x(t+1) - \hat{x}_{AR}(t+1)$ is the error of a linear one-step-ahead prediction $\hat{x}_{AR}(t+1)$ based on the autoregression model of the second order (AR-prediction), whose coefficients are also evaluated over the previous "small" time window with a length of $n$ counts, i.e., the following model is considered:

$$x(t) + a_1 xt - 1 + a_2 x(t-2) = e(t) + d, \qquad (3)$$

in which the vector $c = (a_1, a_2, d)^T$ is the vector of unknown parameters to be determined from the moving "small" window with a length of $n$ counts from the condition of the minimum sum of the squared misfits $e(t)$. I introduce the vector $Y(t) = (-x(t-1), -x(t-2), 1)^T$. Then, the autoregressive model can be written out in the short form as $x(t) = c^T Y(t) + e(t)$. In order to calculate the one-step-ahead prediction $\hat{x}_{AR}(t+1)$, I shall find the vector c from the condition of the minimum sum of the squared misfits $e(t)$ over the previous $n$ counts: $\sum_{\lambda=t-n+3}^{t} e^2(\lambda) = \sum_{\lambda=t-n+3}^{t} (x(\lambda) - c^T Y(\lambda))^2 \longrightarrow \min_c$, from which the formulas for the least square estimates of the vector of parameters and for the one-step-ahead prediction can be easily derived:

$$\hat{c} = A^{-1}t)R(t), \quad A(t) = \sum_{\lambda = t-n+3}^{t} Y(\lambda)Y^T(\lambda),$$
$$R(t) = \sum_{\lambda = t-n+3}^{t} x(\lambda)Y(\lambda), \tag{4}$$
$$\hat{x}_{AR}(t+1) = x(t+1) - \hat{c}^T t)Y(t).$$

The choice of the second order of the autoregression is due to the fact that this is the minimum order for the AR-model, which ensures the description of the vibration's motion and provides the maximum in the spectral density to lie at frequencies between the Nyquist frequency and the zero frequency [Box and Jenkins, 1970; Kashyap and Rao, 1976]. The transition to the increments is necessitated by the need to remove the predominance of low frequencies (the tidal component and the other trends). AR-prediction is based on the property of the correlation between the neighboring increments of the records and, if it is the case, $V_{AR} < V_0$ and $\rho > 0$.

Everywhere below, in the calculation of the index of linear predictability $\rho$ for one-minute data, the estimates were carried out in consecutive "long" time windows with a length of $N = 1440$ counts (24 hours), and also in a "short" time window with a length $n = 60$ counts (one hour).

**Parameters $\alpha$*, $\Delta\alpha$, and $\gamma$ of the multi-fractal spectrum of singularity.** Let $X(t)$ be a random process. I determine the measure $\theta(t, \delta)$ of the behavior of a signal $X(t)$ at the interval $[t, t + \delta]$ as the span $\theta(t,\delta) = \max_{t \le \lambda \le t+\delta} X(\lambda) - \min_{t \le \lambda \le t+\delta} X(\lambda)$ and calculate the mean value of the power $q$ module of such measures:

$$M(\delta,q) = M\{(\theta(t,\delta))^q\}, \tag{5}$$

where M{...} is the sign of mathematical expectation. The random process is called scale-invariant if $M(\delta, q) \sim |\delta|^{\nu(q)}$ at $\delta \longrightarrow 0$, i.e., the limit exists:

$$\nu(q) = \lim_{\delta \to 0} \frac{\ln M(\delta,q)}{\ln|\delta|}. \tag{6}$$

If the dependence $\nu(q)$ is linear $\nu(q) = Hq$, where $H = \text{const}$, $0 < H < 1$, then the process is called monofractal [Taqqu, 1988]. The spectrum of singularity $F(\alpha)$ can be defined as the fractal dimension of the time moments $\lambda_\alpha$, which have the same value of the local Holder–Lipschitz number: $h(t) = \lim_{\delta \to 0} \frac{\ln(\theta(t,\delta))}{\ln|\delta|}$, i.e., $h(\lambda_\alpha) = \alpha$. The raising to different powers $q$ in formula (5) means that this operation allows one to assign different weights to the time intervals with large and small measures of variability of the signal. If $q > 0$, then the main contribution into the mean value $M(\delta, q)$ is provided by time intervals with large variability, whereas the maximum contribution of time intervals with small variability is provided at $q < 0$.

If we evaluate the spectrum of singularity $F(\alpha)$ within the moving time window, then its evolution gives information about the changes in the noise structure. For evaluating the spectrum of a singularity in a moving time window, in the present work I used a kind of the detrended fluctuation analysis (DFA) method [Kantelhardt et al., 2002], which is described in detail in the works [Lyubushin and Sobolev, 2006; Lyubushin, 2007; 2008; 2009]. Below, when analyzing low-frequency microseisms, the estimates of the spectrum of singularity in consecutive nonintersecting time windows with a length of 24 hours (1440 counts) were used; and the local scale-dependent trends were removed by polynomials of the eighth order.

The position and the width of the support of spectrum $F(\alpha)$, i.e., the values $\alpha_{\min}$, $\alpha_{\max}$, $\Delta\alpha = \alpha_{\max} - \alpha_{\min}$, and $\alpha^*$, which is the value providing the maximum of the function $F(\alpha)$, $F(\alpha^*) = \max_\alpha F(\alpha)$, are the characteristics of noise. The value $\alpha^*$ is called the generalized Hurst exponent. For the monofractal signal, the value $\Delta\alpha$ must be zero, and $\alpha^* = H$. Usually, $F(\alpha^*) = 1$, although there are also windows, for which $F(\alpha^*) < 1$. I shall focus mainly on studying the changes in the two parameters of the spectrum of singularity: the generalized Hurst exponent $\alpha^*$ and the width of the support of the spectrum of singularity $\Delta\alpha$. The value $\alpha^*$ characterizes the most typical and frequently occurring Holder–Lipschitz number, whereas $\Delta\alpha$ reflects the diversity in the random behavior of the signal and is a type of measure for the number of latent degrees of freedom of a stochastic system. In addition to these two parameters, I shall also analyze the value $\gamma = \alpha^* - (\alpha_{\min} + \alpha_{\max})/2$, which characterizes the asymmetry of the spectrum of singularity.

Similarly to the designations $\bar{\beta}_r(s)$ and $\overline{\log(Var)}_r(s)$ introduced above, I designate the median values of the corresponding statistics by $\bar{\rho}_r(s)$, $\bar{\alpha}_r^*(s)$, $\overline{\Delta\alpha}_r(s)$, and $\bar{\gamma}_r(s)$, where, the overline means the operation of calculating the median; the argument $s$ enumerates the sequential days, and the index $r = 1, \ldots, 5$ indicates the cluster of stations.

**A robust multiple measure for correlation κ.** In this paragraph I briefly describe the procedure for calculating the measure, which describes the multiple (joint) correlation between the components of multidimensional time series. This procedure is based on the use of canonical correlations [Hotelling, 1936; Rao, 1965], but differs from the classical approach in the use of robust (stable to outliers) estimates. A detailed description of it can be found in the work [Lyubushin, 2007]. Let $u_r(s)$, $r = 1, \ldots, Q$ be the $Q$-dimensional time series, $s = 1, \ldots, L$ be the discrete time. In our case, $Q = 5$ (the number of clusters of stations); $u_r(s)$ are the median daily values $\bar{\beta}_r(s)$, $\overline{\log(Var)}_r(s)$, $\bar{\rho}_r(s)$, $\bar{\alpha}_r^*(s)$, $\overline{\Delta\alpha}_r(s)$, $\bar{\gamma}_r(s)$; $s$ is the index, which enumerates the consecutive days; $L$ is the total number of consecutive days analyzed simultaneously, which will further in the text be either 91 (a quarter of a year) or 365 (one year).

Let us focus on the component with the number $p$ and examine the model of linear regression for the influence of all other components on the selected $u_p$

$$u_p(s) = w_p(s) + \varepsilon_p(s),$$
$$w_p(s) = \sum_{r=1, r \neq p}^{Q} \gamma_r^{(p)} u_r(s). \tag{7}$$

The regression coefficients $\gamma_r^{(p)}$ are found from the condition of the minimum sum of the moduli $\sum_{s=1}^{L} |\varepsilon_p(s)|$, after which I calculate an estimate of the coefficient of correlation $\mu_p$ between the chosen component $u_p(s)$ and the resulting regression contribution of $w_p(s)$ according to the formula of the robust assessment of the coefficient of correlation [Huber, 1981]:

$$\mu_p = (S(\hat{z}_p^2) - S(\check{z}_p^2))/(S(\hat{z}_p^2) + S(\check{z}_p^2)), \tag{8}$$

where $\hat{z}_p(t) = a_p u_p(s) + b_p w_p(s)$, $\check{z}_p(s) = a_p u_p(s) - b_p w_p(s)$, $a_p = 1/S(u_p)$, $b_p = 1/S(w_p)$, $S(u_p) = \mathrm{med}|u_p - \mathrm{med}(u_p)|$. Here $\mathrm{med}(u_p)$ is the median for the sample $u_p(s)$, $s = 1, \ldots, L$, and, thus, $S(u_p)$ is the absolute median deviation of the sample $u_p(s)$. The need for using the robust estimates, i.e., the minimization of the sum of the absolute values of the regression remainders $\varepsilon_p(s)$, rather than their squared values (which is much simpler in terms of computations), and the use of formula (8) for evaluating the coefficient of correlation results from the necessity to provide stability in the obtained estimates $\mu_p$ against the large outliers caused by the arrivals of waves from the close weak and intermediate earthquakes and from the remote strong earthquakes.

The value $\mu_p$ will be called the robust canonical correlation [Hotelling, 1936; Rao, 1965] of the $p$ component with respect to all others. Let us perform these calculations consecutively for all $p = 1, \ldots, Q$. Then, I shall determine the value:

$$\kappa = \prod_{p=1}^{Q} |\mu_p|, \tag{9}$$

which I shall call the robust multiple measure for the correlation of the multidimensional time series.

Evidently, $0 \leq \kappa \leq 1$, and the closer the value (9) to unity, the stronger the general interrelation of the variations in the components of the multidimensional time series $u_p(s)$ with each other. After the calculation of the values (9) not for the entire sample, but within the moving time window of the given length of $L$ counts with the time marker of the right end of the moving window $\tau$, I will estimate the evolution of multiple correlation (9) in the form of dependence $\kappa(\tau|L)$. From the number of the statistics of the daily time segments I will infer six such dependences; when writing them out, I will omit for simplicity the second argument $L$: $\kappa_\beta(\tau)$, $\kappa_{\log(Var)}(\tau)$, $\kappa_\rho(\tau)$, $\kappa_{\alpha*}(\tau)$, $\kappa_{\Delta\alpha}(\tau)$, and $\kappa_\gamma(\tau)$. It should also be noted that the values (8) and (9) were calculated not for the initial data, but for the increments of the median values in order to provide a higher stationarity of the analyzed samples.

## THE RESULTS OF THE ANALYSIS

The graphs of the median values of the six statistics are presented in Figs. 2 and 3. They are characterized by rather random and chaotic patterns of behavior. Thus, the time averages of the initial median values in a moving window with a radius of 14 days are plotted in these figures by the solid black lines. These mean values often exhibit pronounced seasonal (annual) variations. Attention should be paid to the change in the behavior of seasonal variations in the parameters $\bar{\alpha}_r^*$, $r = 1$, 2, and 3 in Fig. 3 after the Hokkaido earthquake: the amplitude of the annual variations significantly decreased. This effect has also been emphasized in the work [Lyubushin, 2009].

I also note that, although the annual variations in the values presented in Fig. 2 are rather synchronous, the general low-frequency trend of the decrease in the median values $\overline{\log(Var)}$ is accompanied by a similar general trend of an increase in the index of linear predictability $\bar{\rho}$. This tendency is most distinct for the fourth and the fifth clusters within the time interval from the end of 2002 to the beginning of 2003. In this

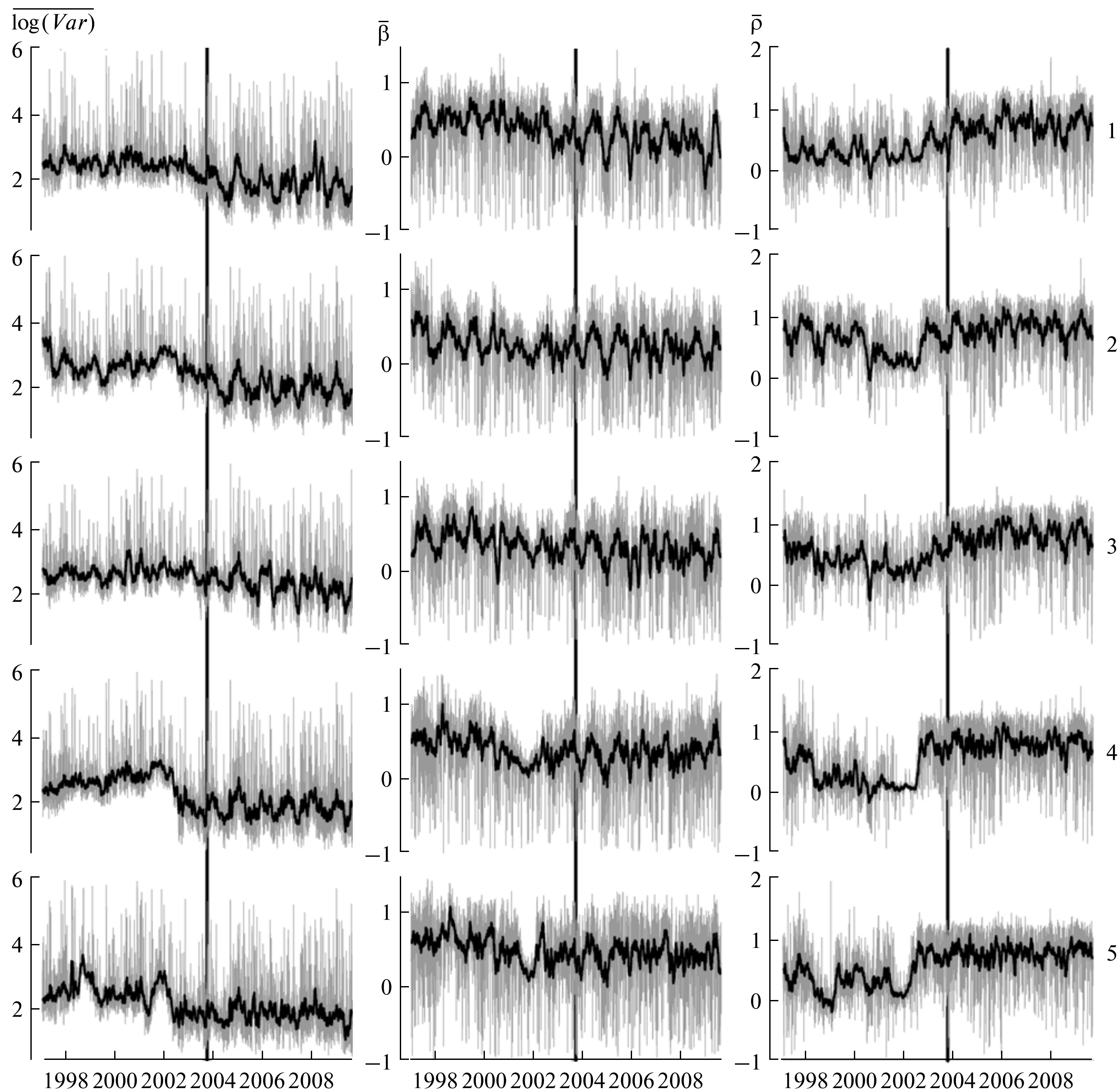


**Fig. 2.** The graphs (gray lines) showing the behavior of the medians of the decimal logarithmic variance $\overline{\log(Var)}$; the spectral exponents $\bar{\beta}$; and the indices of linear predictability $\bar{\rho}$, calculated for stations within five clusters, whose positions are presented in Fig. 1 (the cluster numbers are written to the right of the plots) for the one-minute seismic records. Their averages in a moving time window with a radius of 14 days are depicted by the solid black lines. The parameters were calculated within consecutive time windows with a length of 1440 counts (24 hours). The vertical lines correspond to the time of the earthquake of September 25, 2003.

case, the values $\bar{\rho}_4$ and $\bar{\rho}_5$ undergo a considerable and rather sharp jump, which occurs in July 2002. In all likelihood, this jump can be considered as the beginning of the increase in the synchronization. As it is implied by the construction of the index of linear predictability, an increase in this index indicates an increase in the time correlation of the microseismic vibrations. The median $\bar{\rho}$ increases rather smoothly for the three northern clusters, whereas for the two southern clusters it increases stepwise. The maxima in the medians of the spectral exponents $\bar{\beta}$ often fall on the summer months, and the minimums, on the win-

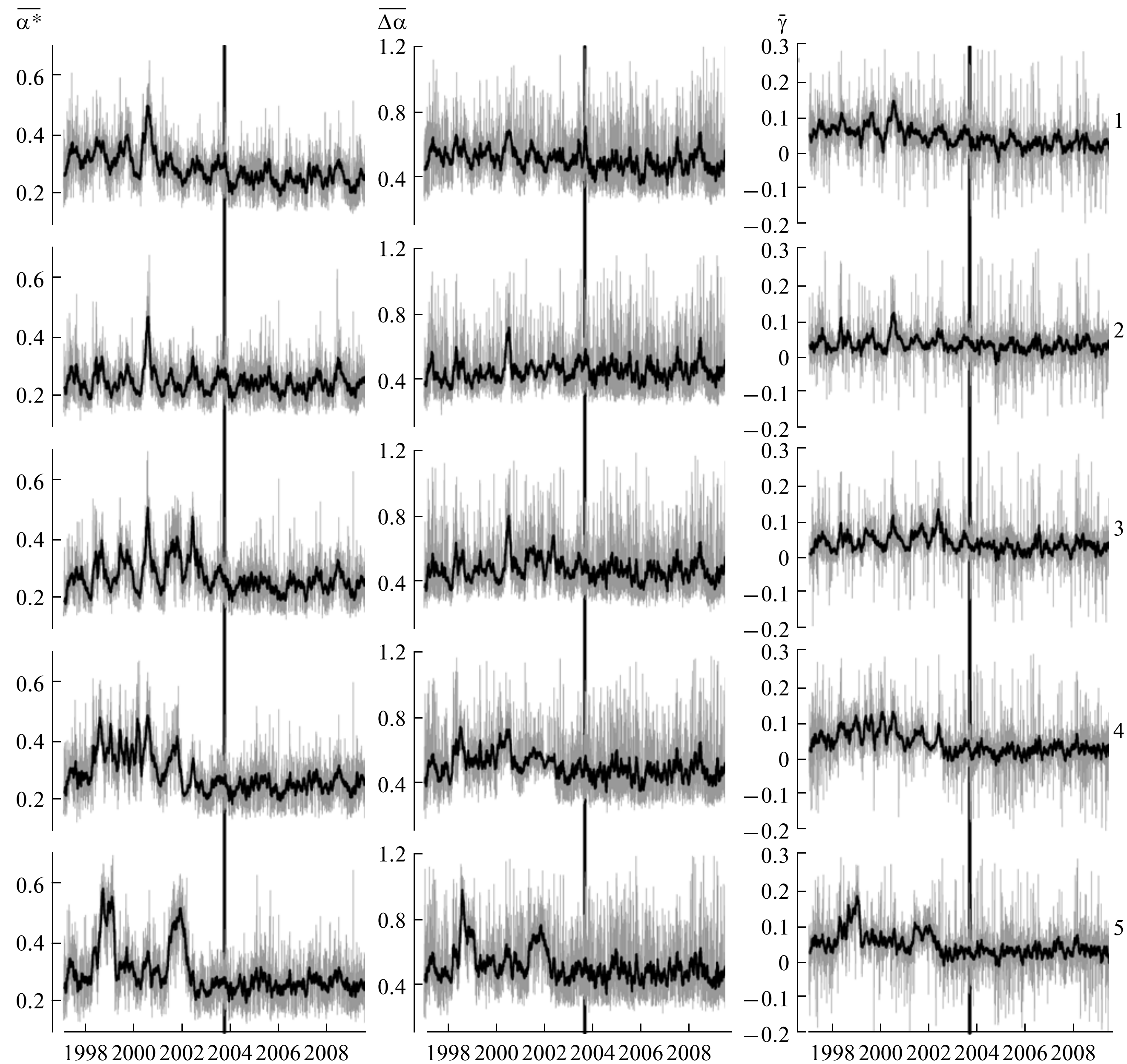


**Fig. 3.** The graphs showing the behavior of the medians of parameters $\overline{\alpha}^*$, $\overline{\Delta\alpha}$, $\bar{\gamma}$ of the multi-fractal spectra of singularity, calculated for stations within five clusters, whose positions are presented in Fig. 1 (the cluster numbers are written to the right of the plots) for the one-minute seismic records are depicted by the gray lines. Their averages in the moving time window with a radius of 14 days are shown by the solid black lines. The singularity spectra were calculated within consecutive time windows with a length of 1440 counts (24 hours). The vertical lines correspond to the time of the earthquake of September 25, 2003.

ter months, i.e., in summer the microseisms have a lower-frequency pattern than in winter.

Figure 4 depicts the changes in the robust multiple measure for correlation κ for all statistics. The measure (9) is calculated for two time windows, 91 and 365 days. It should be noted that the use of a year-long time window for calculating the measure of correlation is equivalent to the averaging of the seasonal impacts of the cyclones, storms, and hurricanes, which are the main sources of generation of low-frequency microseisms; this makes the estimate very smooth and stable, which is noticeable when comparing the gray and the black lines in Fig. 4. The main specific feature of the graphs presented in Fig. 4 is an increase in the power of the coefficient of multiple correlation before the event of September 25, 2003 and its stabilization at the new higher level.

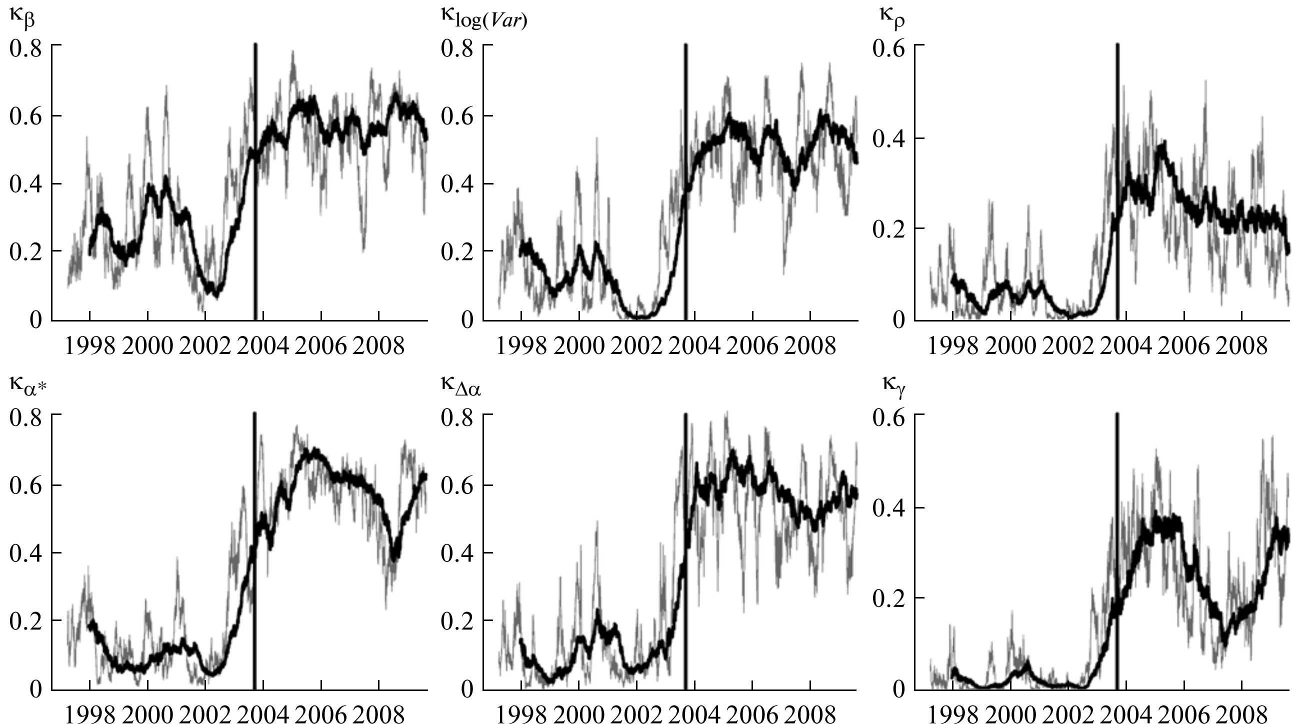


**Fig. 4.** The graphs of the robust multiple measure for correlation κ, evaluated for the increment of the median values of six statistics $\bar{\beta}$, $\overline{\log(Var)}$, $\bar{\rho}$, $\bar{\alpha}^*$, $\overline{\Delta\alpha}$, and $\tilde{\gamma}$ (the subscript of value κ), calculated for the seismic stations within the five spatial clusters (Fig. 1) for one-minute data in the consecutive days. The gray lines correspond to the estimates of κ in the window with a length of 0.25 year (91 counts), and the black lines correspond to the estimates of κ in the window with a length of one year (365 counts). The vertical solid lines correspond to the time of the earthquake of September 25, 2003.

## CONCLUSIONS

The method for calculating spatial averages over the clusters of the observation points of the monitoring systems is developed and implemented. This method allows one to calculate efficiently the measure of correlation and coherence of variations in any statistics, determined on consecutive time intervals in the presence of interruptions in the operation of separate stations.

The analysis showed that the use of time windows with large lengths (one year) makes the identification of the effects of synchronization very stable and statistically significant. This paper presents an independent (based not only on the parameters of the spectra of singularity) validation of the main conclusion of the work [Lyubushin, 2009] about synchronization in the parameters of a low-frequency microseismic field on the Japanese islands related with the Hokkaido earthquake of September 25, 2003; the use of the new statistics, namely the index of linear predictability, allowed me to determine with rather high accuracy the starting time of the systematic increase in the synchronization as July 2002.

## ACKNOWLEDGMENTS

This work was supported by the Program "Electronic Earth" of the Presidium of the Russian Academy of Sciences and by the Russian Foundation for Basic Research, project no. 09-05-00134.

## REFERENCES


1. J. Berger, P. Davis, and G. Ekstrom, "Ambient Earth Noise: A Survey of the Global Seismographic Network," J. Geophys. Res. **109**, B11307 (2004).
2. G. E. P. Box and G. M. Jenkins, *Time Series Analysis. Forecasting and Control* (Holden-Day, San Francisco, 1970; Mir, Moscow, 1974).
3. D. R. Cox and D. V. Hinkley, *Theoretical Statistics* (Chapman and Hall, London, 1974; Mir, Moscow, 1978).
4. G. Currenti, C. del Negro, V. Lapenna, and L. Telesca, "Multifractality in Local Geomagnetic Field at Etna Volcano, Sicily (Southern Italy)," Natural Hazards and Earth System Sciences **5**, 555–559 (2005).
5. G. Ekstrom, "Time Domain Analysis of Earth's Long-Period Background Seismic Radiation," J. Geophys. Res. **106** (B11), 26483–26493 (2001).
6. J. Feder, *Fractals* (Plenum Press, New York, 1988; Mir, Moscow, 1991).
7. A. Friedrich, F. Krüger, and K. Klinge, "Ocean-Generated Microseismic Noise Located with the Grafenberg Array," Journal of Seismology **2** (1), 47–64 (1998).

8. R. Gilmore, *Catastrophe Theory for Scientists and Engineers* (John Wiley and Sons, Inc., New York, 1981; Mir, Moscow, 1984).
9. B. Gutenberg, "Microseisms and Weather Forecasting," Journal of Meteorology, **4** (1), 21–28 (1947).
10. H. Hotelling, "Relations between Two Sets of Variates," Biometrika, **28**, 321–377 (1936).
11. P. J. Huber, *Robust Statistics* (John Wiley and Sons, New York, 1981; Mir, Moscow, 1984).
12. Y. Ida, M. Hayakawa, A. Adalev, and K. Gotoh, "Multifractal Analysis for the ULF Geomagnetic Data during the 1993 Guam Earthquake," Nonlinear Processes in Geophysics, **12**, 157–162 (2005).
13. J. W. Kantelhardt, S. A. Zschiegner, E. Konscienly-Bunde, S. Havlin, A. Bunde, and H. E. Stanley, "Multifractal Detrended Fluctuation Analysis of Nonstationary Time Series," Physica **A316**, 87–114 (2002).
14. R. L. Kashyap and A. R. Rao, *Dynamic Stochastic Models from Empirical Data* (Academic Press, New York, 1976; Mir, Moscow, 1983).
15. N. Kobayashi and K. Nishida, "Continuous Excitation of Planetary Free Oscillations by Atmospheric Disturbances," Nature, **395**, 357–360 (1998).
16. D. Kurrle and R. Widmer-Schnidrig, "Spatiotemporal Features of the Earth's Background Oscillations Observed in Central Europe," Geophys. Res. Lett. **33**, L24304 (2006).
17. E. M. Lin'kov, *Seismic phenomena* (Leningr. Gos. Univ., Leningrad, 1987) [in Russian].
18. E. M. Lin'kov, L. N. Petrova, and K. S. Osipov, "Seismic Gravity Pulsations of the Earth and Atmospheric Disturbances as Possible Precursors of Strong Earthquakes," Dokl. Akad. Nauk SSSR **313** (5), 1095–1098 (1990).
19. A. A. Lyubushin, *Data Analysis of the Systems of Geophysical and Ecological Monitoring* (Nauka, Moscow, 2007) [in Russian].
20. A. A. Lyubushin, "Microseismic Noise in the Low Frequency Range (Periods of 1–300 min): Properties and Possible Prognostic Features," Fiz. Zemli, No. 4, 17–34 (2008) [Izvestiya, Physics of the Solid Earth **44** (4), 275–290 (2008)].
21. A. A. Lyubushin, "Synchronization Trends and Rhythms of Multifractal Parameters of the Field of Low-Frequency Microseisms," Fiz. Zemli, No. 5, 15–28 (2009) [Izvestiya, Physics of the Solid Earth **45** (5), 381–394 (2009)].
22. A. A. Lyubushin and G. A. Sobolev, "Multifractal Measures of Synchronization of Microseismic Oscillations in a Minute Range of Periods," Fiz. Zemli, No. 9, 18–28 (2006) [Izvestiya, Physics of the Solid Earth **42** (9), 734–744 (2006)].
23. S. Mallat, *A Wavelet Tour of Signal Processing* (Academic Press, San Diego, 1998; Mir, Moscow, 2005).
24. A. Ramirez-Rojas, A. Munoz-Diosdado, C. G. Pavia-Miller, and F. Angulo-Brown, "Spectral and Multifractal Study of Electroseismic Time Series Associated to the $M_w = 6.5$ Earthquake of October 24, 1993 in Mexico," Natural Hazards and Earth System Sciences, No. 4, 703–709 (2004).
25. C. R. Rao, *Linear Statistical Inference and Its Applications* (John Wiley, New York, 1965; Nauka, Moscow, 1968).
26. J. Rhie and B. Romanowicz, "A Study of the Relation between Ocean Storms and the Earth's Hum," G3: Geochemistry, Geophysics, Geosystems, An Electronic Journal of Earth Sciences, http://www.agu.org/iournals/gc/, **7** (10), (2006).
27. J. Rhie and B. Romanowicz, "Excitation of Earth's Continuous Free Oscillations by Atmosphere–Ocean–Seafloor Coupling," Nature **431**, 552–554 (2004).
28. V. B. Smirnov and A. V. Ponomarev, Qian Jiadong, and A. S. Cherepanov, "Rhythms and Deterministic Chaos in the Geophysical Time Series," Fiz. Zemli, No. 6, 6–28 (2005) [Izvestiya, Physics of the Solid Earth **41** (6), 428–448 (2005)].
29. G. A. Sobolev, "Series of Asymmetric Pulses in the Low-Frequency Range (Periods of 1–300 min) of Microseisms as Indicators of a Metastable State in Seismically Active Zones," Fiz. Zemli, No. 4, 3–16 (2008) [Izvestiya, Physics of the Solid Earth **44** (4), 261–274 (2008)].
30. G. A. Sobolev, "Microseismic Variations Prior to a Strong Earthquake," Fiz. Zemli, No. 6, 3–13 (2004) [Izvestiya, Physics of the Solid Earth **40** (6), 455–464 (2004)].
31. G. A. Sobolev and A. A. Lyubushin, "Microseismic Anomalies before the Sumatra Earthquake of December 26, 2004," Fiz. Zemli, No. 5, 3–16 (2007) [Izvestiya, Physics of the Solid Earth **43** (5), 341–353 (2007)].
32. G. A. Sobolev and A. A. Lyubushin, "Microseismic Impulses as Earthquake Precursors," Fiz. Zemli, No. 9, 5–17 (2006) [Izvestiya, Physics of the Solid Earth **42** (9), 721–733 (2006)].
33. G. A. Sobolev, A. A. Lyubushin, and N. A. Zakrzhevskaya, "Asymmetric Pulses, Periodicities and Synchronization of the Low-Frequency Microseisms," Vulkanol. Seismol., No. 2, 135–152 (2008).
34. G. A. Sobolev, A. A. Lyubushin, and N. A. Zakrzhevskaya, "Synchronization of Microseismic Variations within a Minute Range of Periods," Fiz. Zemli, No. 8, 3–27 (2005) [Izvestiya, Physics of the Solid Earth **41** (8), 599–621 (2005)].
35. L.Stehly, M. Campillo, and N. M. Shapiro, "A Study of the Seismic Noise from Its Long-Range Correlation Properties," J. Geophys. Res. **111**, Â10306 (2006).
36. T. Tanimoto, "Continuous Free Oscillations: Atmosphere-Solid Earth Coupling," Annu. Rev. Earth Planet. Sci. **29**, 563–584 (2001).
37. T. Tanimoto, "The Oceanic Excitation Hypothesis for the Continuous Oscillations of the Earth," Geophys. J. Int. **160**, 276–288 (2005).
38. T. Tanimoto and J. Urn, "Cause of Continuous Oscillations of the Earth," J. Geophys. Res. **104** (28), 723–739 (1999).
39. T. Tanimoto, J. Urn, K. Nishida, and N. Kobayashi, "Earth's Continuous Oscillations Observed on Seismically Quiet Days," Geophys. Res. Lett. **25**, 1553–1556 (1998).
40. M. S. Taqqu, "Self-Similar Processes," in *Encyclopedia of Statistical Sciences* (Wiley, New York, 1988), Vol. 8, pp. 352–357.
41. L. Telesca, G. Colangelo, and V. Lapenna, "Multifractal Variability in Geoelectrical Signals and Correlations with Seismicity: A Study Case in Southern Italy," Natural Hazards and Earth System Sciences, No. 5, 673–677 (2005).